Tides in the Polar Mesosphere Derived from Two MF Radar Measurements at Poker Flat and Tromsø

NOZAWA Satonori, IWAHASHI Hiroyuki, TSUDA Takuo, OHYAMA Shin-ichiro, FUJII Ryoichi, Chris M. HALL, Alan MANSON, Chris MEEK, Ageir BREKKE, KAWAMURA Seiji, and MURAYAMA Yasuhiro

We have investigated diurnal and semidiurnal tides in the polar mesosphere based on wind data obtained from November 1998 to December 2002 with two MF radars located at Tromsø (69.58˚ N, 19.22˚ E) and Poker Flat (65.1˚ N, 147.5˚ W). We have investigated characteristics of diurnal and semidiurnal amplitudes and phases between 70 and 91 km. Also, we have compared amplitudes and phases of the diurnal and semidiurnal tides at two sites, and investigated contributions of the non-migrating tide of the semidiurnal tide.

Keywords
Tides, Polar mesosphere, MF radar, Zonal wavenumber

1 Introduction

Tides are global-scale waves having cycles of 24, 12, 8, and 6 hours. The sources of tidal generation include (1) heat absorption of solar radiation (mainly ultraviolet radiation), (2) the latent heat effect in the troposphere, (3) interactions between global-scale tides, (4) interactions between tides and atmospheric gravity waves, and (5) solar gravitational effects. Of the above, tides generated by (1) and (5) will be synchronous with the apparent motions of the Sun, and their phases will be dependent on the local time. Thus, these tides are referred to as migrating tides. In contrast, the phases of the tides generated by (2), (3), or (4) will not be synchronized with the apparent motions of the Sun (i.e., with local time), and are referred to as non-migrating tides. Migrating tides may be derived as solutions to classical tidal equations. The semidiurnal tides are westward propagating tides with zonal wavenumber 2. On the other hand, recent model simulations (GSWM) have suggested that non-migrating semidiurnal tides will propagate both in the westward and eastward direction, and will display a variety of characteristics [*Hagan and Forbes,* 2003].

Tides and planetary waves play an important role in the dynamics of the atmosphere in the mesosphere and the lower thermosphere. MF and meteor radars are widely used for studies on such wave propagation in the mesosphere and have produced significant results. Tides and planetary waves are global-scale waves and thus simultaneous observations at multiple points are required to understand their properties. This sort of research has recently been carried out in the middle latitudes, but none so far in the arctic region.

Tromsø (69.6˚ N, 19.2˚ E) and Poker Flat (65.1˚ N, 147.5˚ W) are both located in the arctic region, approximately 167˚ apart at nearly the same latitude. Using the two MF

radars installed at Tromsø and Poker Flat, it should be possible to gain information on the zonal wavenumber of atmospheric waves.

2 Data

A major renewal of the Tromsø MF radar system [*Hall,* 2001] was carried out from the summer to autumn of 1998, and since November 1998, the radar has produced high-quality data at temporal and altitudinal resolutions of 2 to 5 minutes and 3 km. The Tromsø MF radar is managed jointly by the University of Tromsø, University of Saskatchewan, and Nagoya University. The Poker Flat MF radar [*Murayama et al.,* 2000] has been operated by the University of Alaska, Fairbanks and the Communications Research Laboratory (currently NICT) since November 1998. Its altitudinal and temporal resolutions are 4 km (gate interval of 2 km) and 3 sminutes.

Analysis was performed of data acquired from Nov. 1, 1998 to Dec. 31, 2002 by the two radars. The data acquisition method for both radars incorporates Full Correlation Analysis [*Briggs,* 1984; *Meek,* 1980] using Spaced Antennas; we believe there is no system bias between the two. The data were averaged for time and altitude for 1-month blocks. In other words, for the Tromsø data, 24-hour time series data having a temporal resolution of 5 minutes and altitudinal resolution of 3 km were generated, and frequency analysis was performed on these averaged data to determine the components of the diurnal and semidiurnal variations; the resultant values were used to represent the diurnal and semidiurnal tides.

3 Results

3.1 Diurnal tides

Figure 1 shows the monthly and inter-annual variations of diurnal tides (meridional component) at altitudes of 70 and 91 km at Tromsø. The amplitudes of the diurnal tides were small at lower latitudes (approximately 5 m/s) for all seasons. From April to September, the amplitudes tend to increase with altitude and reach about 10 m/s at 91 km. From October to March, there are no significant variations in amplitude with altitude. On the other hand, the inter-annual variations shown here are small.

The characteristics of the diurnal tidal components may be summarized as follows. (1) The amplitude is approximately 15 m/s or smaller and shows similar variations in pattern for the four years in the analysis, although the inter-annual differences may be as high as 8 m/s. The inter-annual differences are minimal in April and October. (2) At an altitude of

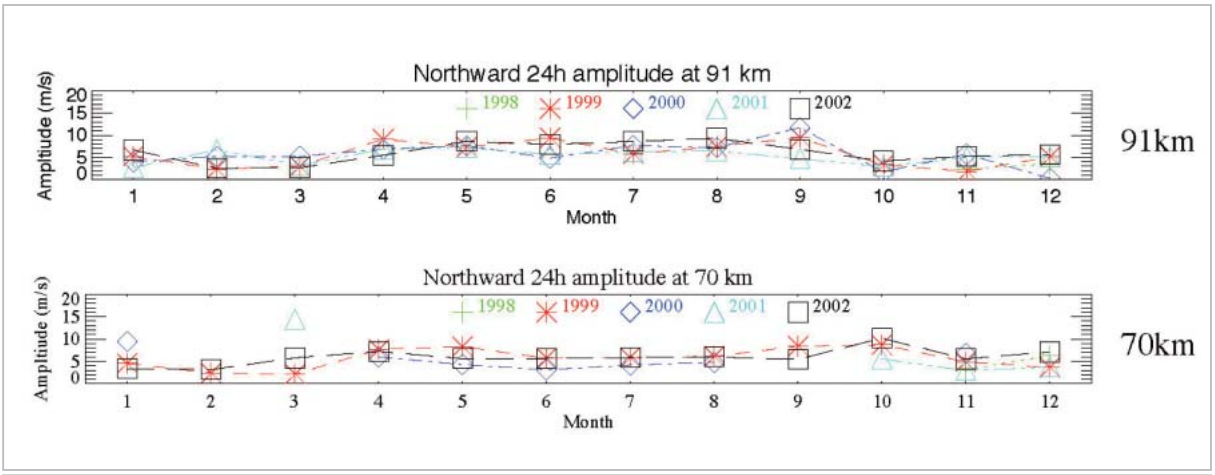

Fig.1 *Seasonal and inter-annual variations in diurnal tides (meridional component) at altitudes of 91 km (top) and 70 km (bottom) above Tromsø*

The cross, asterisk, diamond, triangle, and squares represent data for 1998, 1999, 2000, 2001, and 2002, respectively.

79 km above Tromsø, the amplitudes of both the zonal and meridional components are large (10–15 m/s) in the summer and small (approx. 5 m/s) in the winter. (3) At Poker Flat, the amplitude appears larger during the summer. However, the inter-monthly variations are small, and the amplitude remains relatively stable throughout the year at 5–10 m/s. (4) The meridional components of phase are stable throughout the year, and are located at about 12 o'clock in local time. The inter-annual variations are small. (5) The inter-annual and seasonal variations in the zonal components of phase are both small.

3.2 Semidiurnal tides

Figure 2 shows the temporal variations of semidiurnal tides at two altitudes above Tromsø. At an altitude of 70 km, the intensity of the semidiurnal tide is extremely small for all months (< 3 m/s). The amplitude tends to increase with altitude and reaches 10–20 m/s at 91 km. Intensities of inter-annual variations at an altitude of 70 km are small for all years. In contrast, at 91 km, variations on the order of 5 m/s are observed in many months. At Poker Flat, the amplitudes are 5–10 m/s at an altitude of 70 km. The amplitude tends to increase with altitude, although the increase is not as significant as at Tromsø. At an altitude of 91 km above Poker Flat, the amplitude is approximately 5–20 m/s.

The characteristics of the semidiurnal tidal components may be summarized as follows. (1) The amplitude increases with altitude, and reaches 5 m/s at 70 km and 10–20 m/s at 91 km. (2) At Tromsø, the amplitudes of both the meridional and zonal components peak in September every year. The second-largest peak is observed in the period from January to February. The inter-annual variations are large, and variations as large as 5–10 m/s may be observed. (3) At Poker Flat, the amplitude is also largest in September. For all four years, the minimum intensity is observed in April. (4) At Tromsø, the phase follows a similar pattern for all four years, and the inter-annual differences are 3 hours or less. (5) The inter-annual differences at Poker Flat are small, as in Tromsø. However, a large variation is observed in the month of April.

4 Discussion

4.1 Comparison of the two sites

Here, we will discuss the zonal wavenumber at the two sites based on phase data. The Tromsø MF radar acquires data from an altitude of 70 km in steps of 3 km, while the Poker Flat MF radar acquires data from a 70-km altitude in steps of 2 km. Therefore, we will compare the data at four altitudes (70 km,

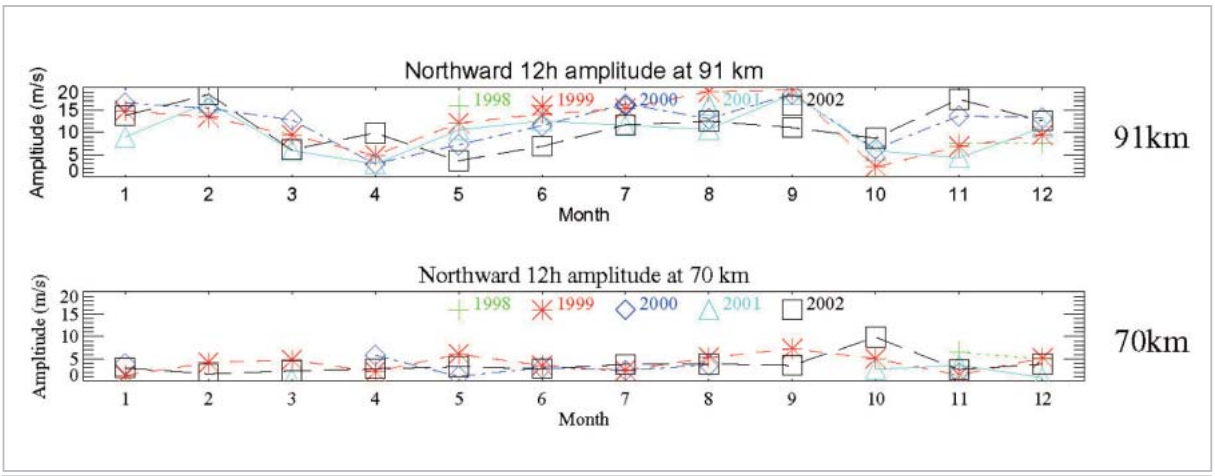

Fig.2 *Seasonal and inter-annual variations in semidiurnal tides (meridional component) at altitudes of 91 km (top) and 70 km (bottom) above Tromsø*

The cross, asterisk, diamond, triangle, and squares represent data for 1998, 1999, 2000, 2001, and 2002, respectively.

76 km, 82 km, and 88 km) common to both radars.

Figure 3 shows a comparison of the amplitude and local time of maximum (hr) at Tromsø and Poker Flat. The horizontal axis represents time (from Nov. 1998 to Dec. 2002), and the data consist of the meridional components for an altitude of 82 km. As stated earlier, the amplitude follows a similar pattern at both sites, and is large in the summer and small in the winter. In contrast, the phase remains stable at noon local time for nearly all months, and there are virtually no differences between the two sites. Similar patterns are observed for the other altitudes. Thus, the presence of a mode having zonal wavenumber 1 is predicted for the diurnal tide. Further, the lack of phase variations in the altitudinal direction indicates the presence of a mode having a significantly high vertical wavenumber. This conclusion in turn implies that the migrating mode propagating upwards from the lower atmosphere has already dissipated and that the in-situ excited mode predominates at altitudes above 70 km.

Figure 4 is a comparison of the meridional components of the semidiurnal tides at an altitude of 82 km above the two sites. The amplitude varies within the range of 5–15 m/s in most cases, and the values of the amplitudes at the two sites do not necessarily coincide. The phases are fairly consistent for the summer season (May to September), but are shifted by about 3–4 hours in the winter. This indicates that the migrating mode predominates in the summer, while contributions from the non-migrating mode cannot be ignored in the winter.

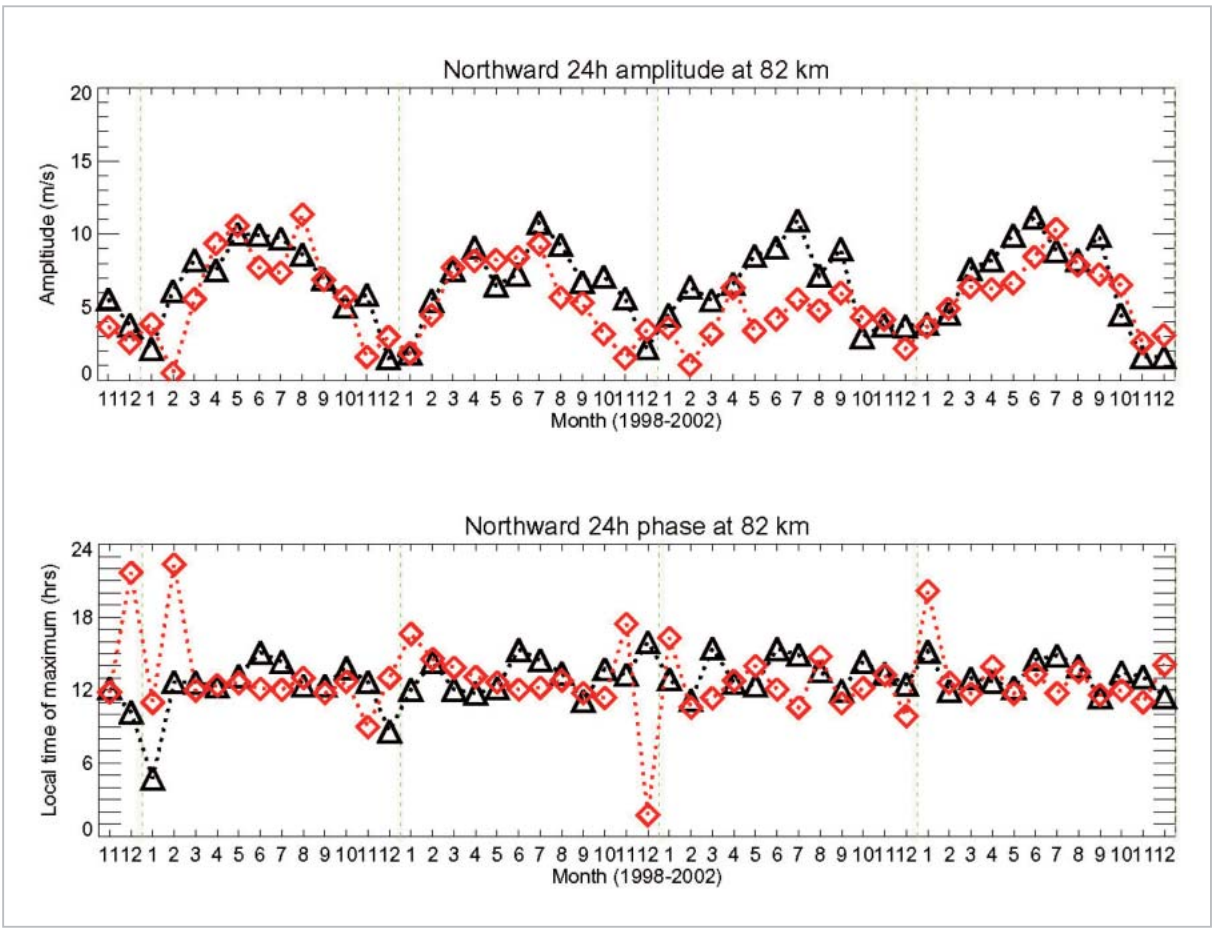

Fig.3 *Comparison of the amplitudes of the diurnal tidal components (meridional components) (top) and phase (bottom) at altitude of 82 km*

Diamonds and triangles represent data at Tromsø and Poker Flat, respectively.

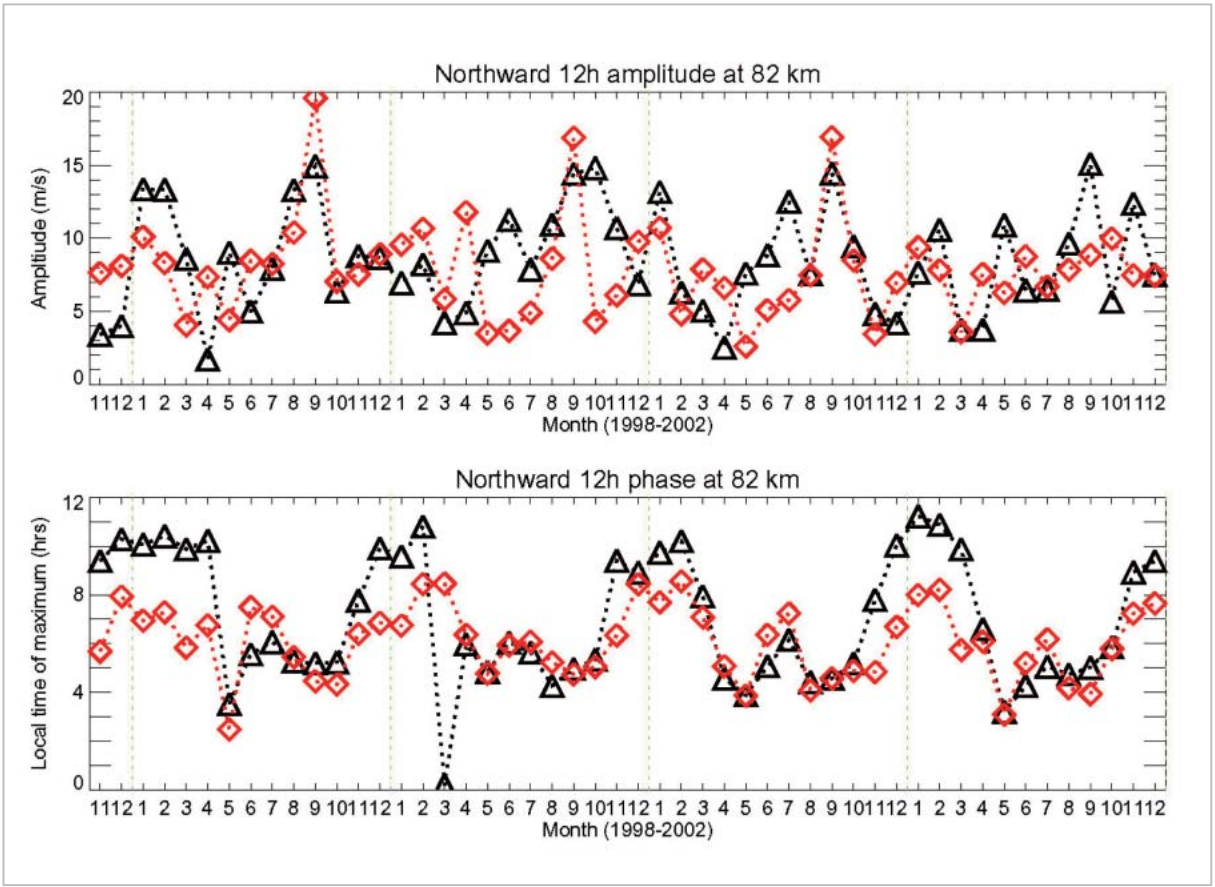

Fig.4 *Comparison of the amplitudes of the semidiurnal tidal components (meridional components) (top) and phase (bottom) at an altitude of 82 km*

Diamonds and triangles represent data at Tromsø and Poker Flat, respectively.

4.2 The non-migrating mode of the semidiurnal tide

In order to perform a more detailed investigation of the characteristics of the semidiurnal tides, 20-day continuous data analysis was performed. The data window covered a period of 20 days, corresponding to the 10 days before and after 1200 UT. The central date in the window was used as the representative day. The waves were separated into modes with zonal wavenumbers of 1 and 2, using the amplitudes and phases of the semidiurnal components satisfying a significance level of at least 99 % at the two sites. In this manner, the frequency analysis and wavenumber separation were performed for the period from Jan. 10, 1999 to Dec. 21, 2002 by shifting the 20-day window by one day at a time.

4.2.1 Wavenumber separation

Generally, the oscillating motion of a semidiurnal tide component observed at one site is a wave synthesized from several semidiurnal tides having varying zonal wavenumbers. Here, we will examine a case that involves semidiurnal tides having two types of zonal wavenumbers.

$$A_1 e^{i[\sigma t_L + s_1\lambda - \phi_1]} + A_2 e^{i[\sigma t_L + s_2\lambda - \phi_2]} = A(\lambda) e^{i[\sigma t_L - \phi(\lambda)]}$$

Here, A, t_L, λ, and ϕ are amplitude, local time, longitude, and phase, respectively, and σ is the frequency. For semidiurnal tides, $\sigma = \pi/12$. The longitudes of Tromsø and Poker Flat are 19.2° E and 147.6° W, respectively. The two terms on the left-hand side of the equation represent the oscillation at longitude λ of the waves having two different zonal wavenumbers, and the right-hand side represents the oscillation observed at the two points.

For the waves having varying zonal

wavenumbers, two values must be selected arbitrarily. *Murphy et al.* [2003] have suggested the presence of a semidiurnal tide having wavenumber 1 based on observations at three sites in the Antarctic region [Davis (68.6° S, 78.0° E, Syowa (69.0° S, 39.6° E), and Rothera (67.6° S, 68.1° W)]. According to calculations using the GSWM model simulations, a westward-propagating wave having zonal wavenumber 1 predominates as the secondary wave [*Hagan and Forbes,* 2003]. Thus, in the present case, we have selected the zonal wavenumbers 1 and 2 ($s_1 = 1$, $s_2 = 2$). By substituting $\lambda = \lambda_{tromso}$ and $\lambda = \lambda_{pokerFlat}$ for Tromsø and Poker Flat, respectively, we have

$$A_1 e^{i[\sigma t_L + s_1 \lambda_{tromso} - \phi_1]} + A_2 e^{i[\sigma t_L + s_2 \lambda_{tromso} - \phi_2]} = A(\lambda_{tromso}) e^{i[\sigma t_L - \phi(\lambda_{tromso})]}$$

$$A_1 e^{i[\sigma t_L + s_1 \lambda_{PokerFlat} - \phi_1]} + A_2 e^{i[\sigma t_L + s_2 \lambda_{PokerFlat} - \phi_2]} = A(\lambda_{PokerFlat}) e^{i[\sigma t_L - \phi(\lambda_{PokerFlat})]}$$

From these two equations, we may obtain

$$A_1 e^{-i\phi_1} = \frac{A(\lambda_{tromso}) e^{-i[2\lambda_{tromso} + \phi(\lambda_{tromso})]} - A(\lambda_{PokerFlat}) e^{-i[2\lambda_{PokerFlat} + \phi(\lambda_{PokerFlat})]}}{e^{-i\lambda_{tromso}} - e^{-i\lambda_{PokerFlat}}}$$

and so we may calculate (A_1, ϕ_1). Similarly, (A_2, ϕ_2) may be calculated. By assuming the two zonal wavenumbers in the above fashion, we are able to determine the amplitudes and phases of the modes from the semidiurnal tide components observed at the two sites by wavenumber separation. In the case where the migrating tide is a semidiurnal tide, the modes will each be westward-propagating with $s = 2$, from classical theory of tides. In contrast, in the case of non-migrating tides, eastward-propagating modes may exist as well as westward-propagating modes, and various zonal wavenumbers may be obtained. However, the wavenumber was assumed to be $s_1 = 1$ here. The zonal wavenumber of $s_2 = 2$ corresponds to the migrating tide and $s_1 = 1$ corresponds to the non-migrating tide.

4.2.2 On the component having zonal wavenumber 1

Figure 5 shows the seasonal variations in amplitude and phase for the wave component having zonal wavenumber 1 for the period of four years from Jan. 1999 to Dec. 2002. The horizontal and vertical axes represent time by month and amplitude, respectively. The years are distinguished by color. From top to bottom, the panels represent the amplitudes and phases at altitudes of 88, 82, 76, and 70 km. At 88 km, maximums in amplitudes are observed from September to October every year for the four years (15–20 m/s). However, the timing of the peak varies from year to year, and dramatic variations within a short period of several days are observed, which cause sudden increases/decrease in amplitude. Except for 1999, increases in amplitude are observed from Nov. to Dec. (by about 10 m/s). At 82 km, the maximum amplitude appears in September, reaching approximately 10 m/s. In addition, maximums (of about 12 m/s) are also observed in winter (Dec. and Jan.). At 76 km, seasonal variations are not particularly marked, but bursts of increased amplitude are occasionally observed, as in April 1999. Almost no seasonal variations are observed at 70 km, and the amplitudes of these variations are 5 m/s or smaller throughout the four-year period.

The diurnal variations in phase are small in summer and winter, while variations with cycles of several days are observed during the periods from March to April and September to October. While inter-annual variations are small for altitudes of 70 and 88 km, they are relatively marked at 76 and 82 km.

The results of MF radar observation at an altitude of 86 km in the Antarctic region (Davis, Syowa, Rothera) *[Murphy et al.,* 2003] show that the non-migrating mode is large during the summer (December to March), with amplitudes of 15–20 m/s. However, the results of our observations for an altitude of 88 km displayed in the panel in Fig. 5 showed a maximum (15–20 m/s) from September to October, with relatively small amplitudes in the summer (5–10 m/s).

4.2.3 On the component having zonal wavenumber 2

Figure 6 shows the seasonal variations in amplitude and phase for components having zonal wavenumber 2. The format is the same as for Fig. 5. The amplitudes of the wave component having wavenumber 2 generally tend

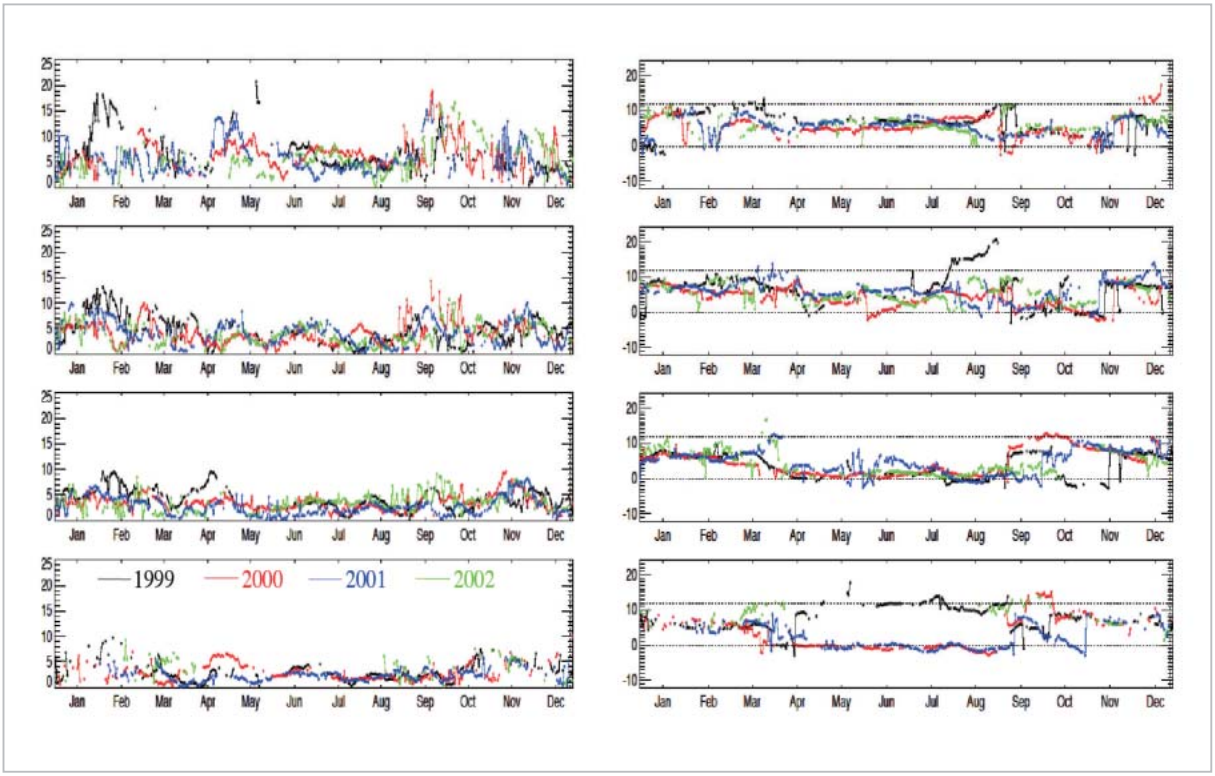

Fig.5 *Seasonal variations in amplitude (left panels) and phase (right panels) for components with zonal wavenumber 1. The horizontal and vertical axes represent time (in months) and amplitude (m/s)/phase (hour), respectively*

From top to bottom, the data are for altitudes of 88, 82, 76, and 70 km.

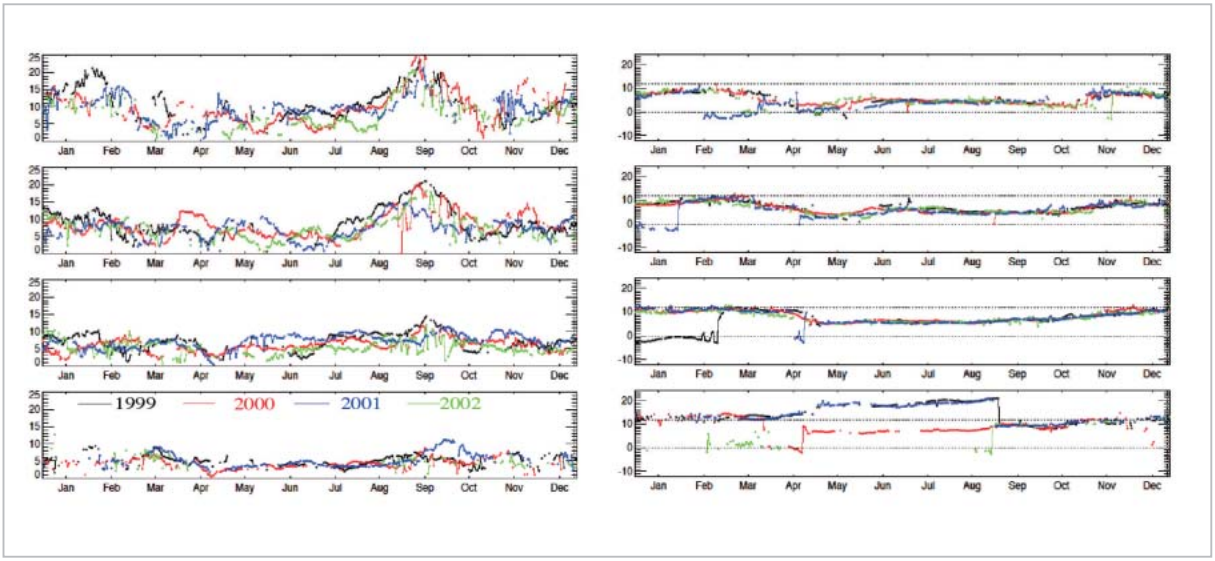

Fig.6 *Seasonal variations in amplitude (left panels) and phase (right panels) for components with zonal wavenumber 2*

From top to bottom, the data are for altitudes of 88, 82, 76, and 70 km.

to increase with altitude throughout the year. In terms of seasonal dependency by altitude, maximums are observed around September (15–25 m/s) and in winter (15–20 m/s) at an altitude of 88 km. However, the amplitudes in the winter display stronger inter-annual variations compared to those in September. At 82 km, peaks are also observed around September, with amplitudes exceeding 15 m/s. In contrast, the seasonal variations and inter-

annual variations are weak at 70 and 76 km, and amplitudes remain nearly constant at 5–10 m/s.

At any altitude, diurnal variations in phase are very small, and almost no intra-annual variations are observed. Phases in summer and winter are almost constant, their variations being 5–6 hours. The higher the altitude, the more the phases tend to lag.

4.2.4 Comparison of the intensities of wave components having wavenumbers 1 and 2

Figure 7 is a comparison of the amplitudes for components with wavenumbers 1 and 2. The horizontal and vertical axes represent time in months and the amplitude ratios. Ratios larger than 1 signify that the amplitude of the migrating tide is larger than that of the non-migrating tide. The solid black line shows the averaged ratio for the four-year period. At all four altitudes (70, 76, 82, and 88 km), the migrating tide is larger in the average value. However, the ratios display strong diurnal variations, and there are periods during which the non-migrating tide significantly predominates. No seasonal variations are observed during this period. Therefore, when performing case studies in these altitude regions, the effect of the non-migrating tide must be accounted for. However, the interesting question of how the non-migrating tide propagates to the lower thermosphere has yet to be resolved.

4.2.5 Vertical wavelength of the migrating tide

The representative mode of the semidiurnal tide calculated from the theory of tides are (2, 2), (2, 3), (2, 4), (2, 5), and (2, 6), and the vertical wavelengths are estimated to be 311, 81.4, 53.8, 41.0, and 33.4 km, respectively [*Forbes,* 1995]. The vertical wavelengths in mesospheric altitudes are short, and the (2, 4) mode is believed to predominate [*Virdi et al.,* 1986, *Williams and Virdi,* 1992]. Therefore, we have classified the events identified for the migrating tides at the four altitudes (70, 76, 82, and 88 km) in the 18-km range into a "long wavelength mode" having phase changes lasting 2 hours or less and a "short wavelength mode" having changes lasting 2–12 hours.

Figure 8 is a histogram of the classification results for the meridional components by season. In each bar, the cyan, magenta, and black correspond to the "long wavelength mode", "short wavelength mode", and "non-upward-propagating events". The data are for the entire four-year period, and the vertical axis represents the proportion of a given event

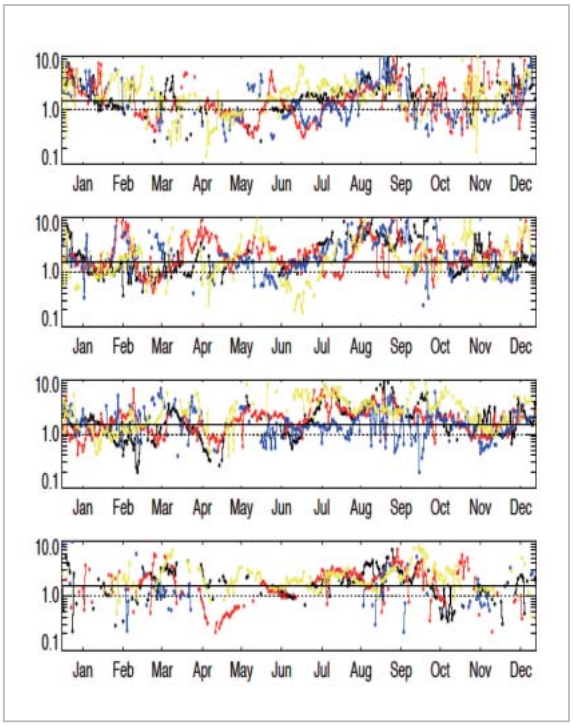

Fig.7 *Amplitude ratios of the migrating tide and the non-migrating tide*

From top to bottom, the data are for altitudes of 88, 82, 76, and 70 km.

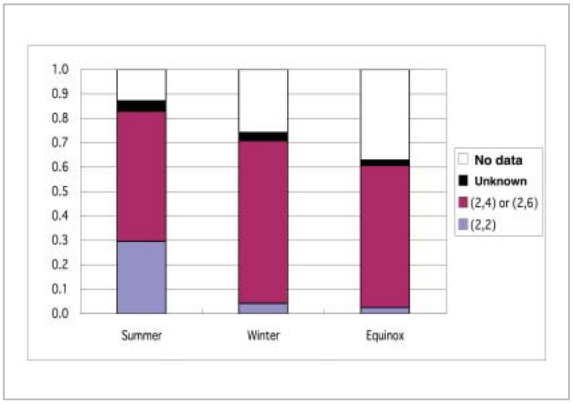

Fig.8 *Distribution of vertical wavelength*

to the whole. For all seasons, upward-propagating events dominate (60–80 %). Of the upward-propagating events, the short wavelength mode is more predominant than the long wavelength mode. However, in the summer, the proportion of the long-wavelength mode reaches 30 %. Such seasonal variations are believed to reflect the interactions between background winds.

5 Conclusions

The characteristics of the diurnal and semidiurnal tides in the polar mesosphere (altitudes of 70–91 km) have been summarized based on the wind velocity data collected by the MF radars at Tromsø (69.6° N, 19.2° E) and Poker Flat (65.1° N, 147.5° W). The amplitudes of the diurnal tides displayed seasonal variations that become marked during the summer. No phase dependency on season or altitude is observed, and the phase remains nearly constant at 12 o'clock. The amplitudes of the semidiurnal tides tended to increase with altitude. Based on a comparative study of the data from the two sites, it has been concluded that the in-situ mode having zonal wavenumber 1 predominates in the diurnal tide. No significant differences are observed in the semidiurnal tide phases of the two sites during the summer, although phase differences on the order of several hours are observed during the winter. This may indicate that the migrating mode is dominant in the summer, while the effects of the non-migrating mode contribute to a significant degree in the winter, in addition to the effects of the migrating mode. Based on phase difference between the two sites, wavenumber separation was performed for components having zonal wavenumbers of 1 and 2, in order to investigate the seasonal variations of each component. Results of comparison of the amplitudes of the two components indicated that there are periods in which the non-migrating tide (assumed to be $s = 1$) predominates over the migrating mode, which suggests the importance of the non-migrating tide in the polar mesosphere.

References

1 Briggs, B. H., "The analysis of spaced sensor records by correlation techniques", Handb. MAP, 13, 166-186, 1984.

2 Forbes, J. M., "Tidal and Planetary Waves", The Upper Mesosphere and Lower Thermosphere: A Review of Experiment and Theory in Geophysical Monograph, Edited by R. M. Johnson and T. L. Killeen, 356 pp, American Geophysical Union, 67-87, 1995.

3 Hagan, M. E. and Forbes, J. M., "Migrating and nonmigrating semidiurnal tides in the upper atmosphere excited by tropospheric latent heat release", J. Geophys. Res., 108, 1062, doi: 10.1029/2002JA009466, 2003.

4 Hall, C. M., "The Ramfjordmoen MF radar (69° N, 19° E): Application development 1990-2000", J. Atmos. Sol.-Terr. Phys., 63, 171-179, 2001.

5 Hocke, K., "Phase estimation with the Lomb-Scargle periodogram method", Ann. Geophys., 16, 356-358, 1998.

6 Meek, C. E., "An efficient method for analyzing ionospheric drifts data", J. Atmos. Terr. Phys., 42, 835-839, 1980.

7 Murayama, Y., K. Igarashi, D. D. Rice, B. J. Watkins, R. L. Collins, K. Mizutani, Y. Saito, and S. Kainuma, "Medium Frequency Radars in Japan and Alaska for Upper Atmosphere Observations", IEICE Trans. Commun., E83-B, 1996-2003, 2000.

8 Murphy, D. J., M. Tsutsumi, D. M. Riggin, G. O. Jones, R. A. Vincent, M. E. Hagan, and S. K. Avery, "Observations of a nonmigrating component of the semidiurnal tide over Antarctica", J. Geophys. Res., 108, 4241, doi: 10.1029/2002JD003077, 2003.
9 Virdi, T. S., G. O. L. Jones and P. J. S. Williams, "EISCAT observations of the E-region semidiurnal tide", Nature, 324, 354-356, 1986.
10 Williams P. J. S. and T. S. Virdi, "Incoherent scatter observations of tides in the lower thermosphere at high latitudes", Advances in Space Research,12, 97-106. 1992.

***NOZAWA Satonori**, Ph.D.*
Associate Professor, Solar Terrestrial Environment Laboratory, Nagoya University
Upper Atmosphere Physics

IWAHASHI Hiroyuki
Solar Terrestrial Environment Laboratory, Nagoya University
Upper Atmosphere Physics

TSUDA Takuo
Solar Terrestrial Environment Laboratory, Nagoya University
Upper Atmosphere Physics

***OHYAMA Shin-ichiro**, Dr. Sci.*
Professor, Solar-Terrestrial Environment Laboratory, Nagoya University
Upper Atmosphere Physics

***FUJII Ryoichi**, Dr. Sci.*
Professor, Director of Solar Terrestrial Environment Laboratory, Nagoya University
Upper Atmosphere Physics

***Chris M. HALL**, Ph.D.*
Professor, University of Tromsø
Upper Atmosphere Physics

***Alan MANSON**, Ph.D.*
Professor, University of Saskatchewan
Upper Atmosphere Physics

***Chris MEEK**, Ph.D.*
Research Associate, University of Saskatchewan
Upper Atmosphere Physics

***Ageir BREKKE**, Ph.D.*
Professor, University of Tromsø
Upper Atmosphere Physics

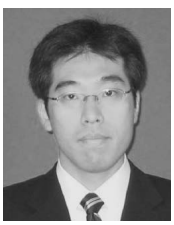

***KAWAMURA Seiji**, Ph.D.*
Researcher, Environment Sensing and Network Group, Applied Electromagnetic Research Center
Atmospheric Physics, Radar Engineering

***MURAYAMA Yasuhiro**, Dr. Eng.*
Planning Manager, Strategic Planning Office, Strategic Planning Department
Dynamics in the Thermosphere and Mesosphere